Korean J. Chem. Eng., 40(12), 3017-3028 (2023)
DOI: 10.1007/s11814-023-1567-z

pISSN: 0256-1115
eISSN: 1975-7220

Exergoeconomic analysis of an LNG integrated - air separation process

Muhammad Haris Hamayun*,, Naveed Ramzan*, and Muhammad Faheem*,†**

*Department of Chemical Engineering, University of Engineering and Technology, Lahore 54890, Pakistan
**Catalysis and Reaction Engineering Research Group, Department of Chemical Engineering, COMSATS University Islamabad, Lahore Campus, Defence Road, Lahore 54000, Pakistan
(*Received 12 July 2023 • Revised 1 September 2023 • Accepted 2 September 2023*)

Abstract−An integrated LNG regasification - air separation process is investigated using exergy and exergoeconomic analyses. The objective of developing this integrated process is to lower the calorific value of LNG by mixing regasified LNG with high purity nitrogen, while simultaneously recovering and utilizing valuable cryogenic energy from the LNG during its regasification to minimize the power consumption of the air separation unit (ASU) for nitrogen production. The overall exergy efficiency and exergy destruction of the integrated process are 76.47% and 28.52 MW, respectively, with the compression section causing the most exergy destruction. Further exergoeconomic analysis of the proposed process reveals that the air compressors have the highest capital investment (CI) and operating and maintenance (O&M) cost rates, the pumps for cooling water and LNG have the highest exergoeconomic factors, and the low-pressure column and a multistream heat exchanger have the highest exergy destruction cost rates. A parametric study is also conducted to examine the impact of economic variables including interest rate, plant life, and compressor performance on exergy destruction, CI and O&M cost rates, and exergoeconomic factor. The findings of this study offer valuable insight into the design and optimization of similar integrated processes, with potential benefits for the energy industry.

Keywords: Exergy Analysis, Exergoeconomic Analysis, LNG Regasification, Air Separation Unit, Process Simulation, Process Integration

INTRODUCTION

Natural gas has the lowest carbon footprint of all fossil fuels [1,2]. Because indigenous natural gas supplies are rapidly declining in many countries, including Pakistan, importing liquefied natural gas (LNG) could be a viable solution to this problem [3,4]. According to ExxonMobil's assessment on the energy outlook, LNG trade is predicted to triple over the next three decades [5]. Natural gas is widely used in Pakistan for both industrial and domestic purposes. However, due to an acute shortage of indigenous natural gas and the possibility of resource exhaustion by 2030, attention has shifted toward the import of LNG from other countries [6,7].

Of the 63.3 trillion cubic feet recoverable natural gas reserves in Pakistan, 42.4 trillion cubic feet had been produced till 2021 [8]. The remaining recoverable natural gas reserves are only 20.9 trillion cubic feet, which is approximately 0.2% of the global proven natural gas reserves [9]. In 2022, 153.9 TWh of electricity was produced in Pakistan, of which 16.3 TWh (10.6%) was produced from indigenous natural gas whereas 31.3 TWh (20.3%) was produced from imported LNG [10].

LNG has a volume approximately 600 times smaller than natural gas, allowing for its easy storage and long-distance transport [11, 12]. LNG is transported in cryogenic containers by sea ships under low pressure (0.13-0.14 MPa) and at cryogenic temperatures (about 100 K) [13,14]. LNG is regasified and brought to the desired operational conditions at LNG terminals before injecting into gas pipelines [13,15-17]. Natural gas cooling and liquefaction processes consume a significant amount of energy. For example, approximately 300 kWh of electrical energy is required to produce 1 ton of LNG. The LNG can therefore be considered as a storage medium for this cryogenic energy [11,16,18]. For LNG vaporization/regasification, submerged combustion vaporizers (SCV) and open rack vaporizers (ORV) are commonly employed [19,20]. However, due to vaporization at ambient temperatures (around 20 °C), the LNG vaporization/regasification process results in the loss of important cryogenic energy, i.e., 240-250 kWh of usable cryogenic energy per ton of regasified LNG [21].

Various approaches for recovering this cryogenic energy from LNG have been proposed in the literature. For example, the power required for seawater desalination can be reduced by using LNG cryogenic energy [15,22]. Similarly, attaching LNG vaporizers to cold storage systems in the food business can lower the power requirements for refrigeration [23]. Liquid CO_2 is required by the agri-food businesses and hypermarkets. Utilizing LNG cryogenic energy can help reduce the power needed to produce liquid CO_2. The LNG regasification process can also be integrated to lower the power consumption of the air separation process [24,25]. The efficiency of the direct expansion cycle for power production can be improved by using LNG as the working fluid. LNG can also be used as the low-temperature medium in the organic Rankine cycle, as well as in Brayton and Kalina cycles [11].

Some existing natural gas fired power plants in Pakistan require the gross calorific value (GCV) of LNG to be between 950-1,000 BTU/scf [26]. On the other hand, the LNG imported in Pakistan

†To whom correspondence should be addressed.
E-mail: faheem@uet.edu.pk

typically has a GCV of 1,050-1,200 BTU/scf, which must be reduced to meet the technical specifications of these gas fired power plants. This can be achieved by mixing LNG with an inert gas, such as nitrogen which can be obtained from the air separation unit (ASU). Mehrpooya et al. [20,27] have previously shown that cryogenic energy recovery by thermal integration of LNG regasification with an ASU is a viable solution based on energy consumption and environmental risks. In particular, the following advantages can be realized by integrating the two processes: (1) The air separation process operates at cryogenic temperatures and consumes significant power in the refrigeration cycle. This power demand can be significantly lowered by using LNG cryogenic energy [28-30]. (2) Mixing LNG with nitrogen reduces the calorific value of LNG. Cryogenic air separation is the most economical industrial scale process for producing large quantities of high purity nitrogen [31].

To reduce the need for external utilities, the conventional air separation process employs a two-column configuration in which both the high- and low-pressure columns (HP and LP columns, respectively) are heat-integrated. The HP column's condenser is heat-integrated with the LP column's reboiler [32]. The normal boiling point of nitrogen (−195.7 °C) is lower than that of oxygen (−183.2 °C). However, by manipulating the pressures of the two columns, it becomes possible to use the condensation heat of nitrogen (HP column) for oxygen vaporization (LP column), thus eliminating the need for external utilities. However, both columns should run at a significant pressure difference to ensure adequate process integration and proper heat exchange between them [33]. As a result, the two-column configuration consumes significant amount of power in the compression section [34,35]. By recovering the cryogenic energy of LNG, the power requirement of the ASU can be decreased in two ways: (1) by cooling the feed air, and (2) by decreasing the power required for air compression [36].

Exergy analysis has been widely used to assess the performance of different chemical processes, including the integrated LNG regasification - air separation process. Exergy-based methods provide a systematic mechanism for identifying process irreversibilities and improving the overall process efficiency by determining optimal operational parameters [37-42].

Xu et al. [43] developed a novel integrated process to recover LNG cryogenic energy and used exergy analysis to compare the proposed process with a conventional LNG-integrated ASU process. They reported that by harnessing cryogenic energy from LNG in the improved design, the compressor power consumption was lowered, resulting in a drop in the HP column pressure from 5 to 3.5 bar. The modified design showed 42.47% improvement in the overall exergy efficiency and 12.6% reduction in the power consumption. Morosuk et al. [44] used exergy analysis to compare an integrated LNG-ASU process with a standalone ASU. The exergy efficiency of the integrated process was enhanced by 11.76% whereas the power consumption was lowered by 40.9% because of efficient utilization of LNG cryogenic energy. Jieyu et al. [45] compared an LNG-integrated ASU with a standalone ASU using exergy analysis. They reported that for the integrated process, the exergy efficiency was increased by 50.5% whereas the power consumption was lowered by 39.1%. The overall exergy efficiency of the combined process was reported to be 57.5%.

In another study, Mehrpooya et al. [46] designed and evaluated an LNG-integrated ASU process using exergy analysis. The impact of various operational parameters, including nitrogen compression pressure, LNG intake temperature, LNG flow rate, turbine inlet temperature, and column operating conditions, on process efficiency was studied using sensitivity analysis. The LNG-integrated process outperformed the standalone process in terms of reduced power requirement and increased energy and exergy efficiencies by 38.5%, 59.4%, and 67.1%, respectively. Ebrahimi and Ziabasharhagh [16] used thermodynamic and economic analyses to analyze the performance of an LNG-integrated ASU process. They reported that efficient utilization of LNG cryogenic energy achieved the following benefits: (1) the power requirement was reduced by 8.04%, (2) the multistream heat exchanger's LMTD was increased by 3 K, thus reducing the required surface area, (3) the initial investment rate was reduced by 17.05%, and (4) the payback period was shortened by one year. Esfilar et al. [47] designed an air separation process that was integrated with LNG regasification and a coal and biomass co-gasification power production cycle. Pure oxygen obtained from the ASU was used as the gasifying agent. Sensitivity analysis was performed on several operational parameters, including coal mass flow rate, fuel composition, biomass/coal ratio, turbine efficiency, and LNG mass flow rate, to increase the overall process efficiency. They reported that the exergy efficiency of the integrated process is 97%, with an exergy destruction of 1,007 MW. The heat exchangers were found to be a major source of exergy destruction.

Exergoeconomic analysis combines exergy and economic evaluations to offer a comprehensive assessment of a process. Three essential components are estimated during this analysis: relative cost difference, exergoeconomic factor, and cost of exergy destruction. Optimization is often based on the exergoeconomic factor [27,48-51]. Mehrpooya and Zonouz [50] combined an ASU with LNG regasification and oxy-combustion CO_2 power cycle and performed an exergoeconomic analysis of the proposed process. The integrated process was reported to have a 67.1% exergy efficiency and 19.3 GW exergy destruction. Sensitivity analyses were performed with respect to interest rate (%), plant life (hours), and turbine efficiency (%). The exergoeconomic and sensitivity analyses suggested that the multistream heat exchanger and LNG pump's operability should be improved. In another work based on exergy and exergoeconomic analyses, Mehrpooya et al. [42] examined a two-column ASU integrated with the LNG regasification process and CO_2 power cycle. They identified the air compressors and one of the multistream heat exchangers as major sources of exergy destruction in the process. Furthermore, they concluded that the individual equipment performance should be improved, or the equipment should be replaced with more efficient models to minimize the overall cost of the process.

In our recent work [33], we have proposed a new approach to integrate the LNG regasification process with the air separation process for recovering the LNG cryogenic energy while simultaneously manipulating the GCV of the LNG by mixing it with the high purity nitrogen produced by the ASU. In the present study, we expand on our previous work by further analyzing the integrated process using exergy and exergoeconomic analyses. A parametric study is also performed to evaluate the impact of the interest rate (%), plant life

(years), and compressor efficiency (%) on the overall process.

MODEL DEVELOPMENT

Aspen Plus® V10 was used to develop a steady-state simulation model of the integrated process using the Peng-Robinson property package [52]. The use of Peng-Robinson property package for modeling air separation processes has been widely reported in the literature [42,43,46]. A schematic diagram of the integrated process is presented in Fig. 1. Because the proposed process has been de-

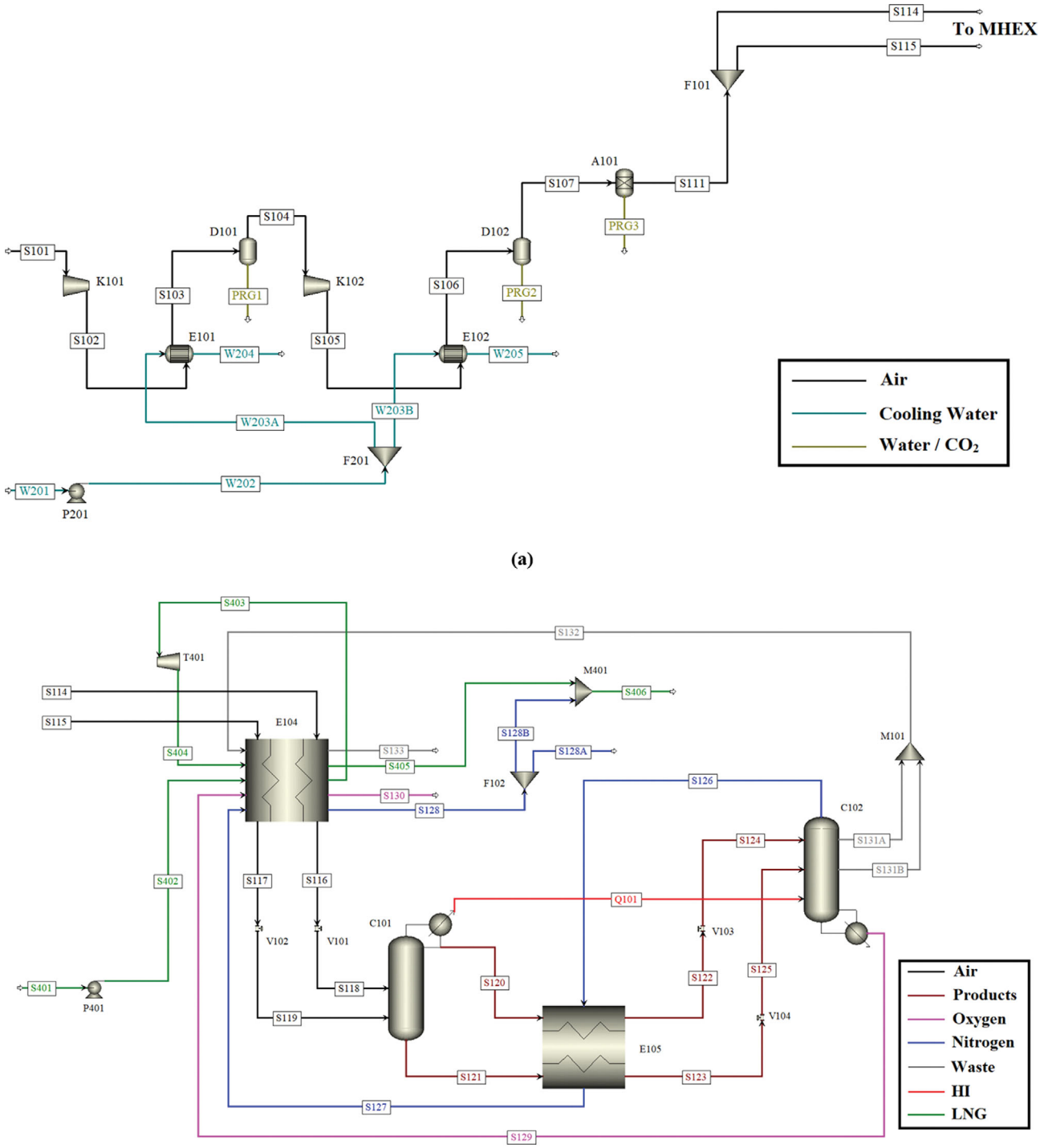

Fig. 1. Schematic of the integrated process (a) compression section, (b) cryogenic section [Reprinted with permission from [33]. Copyright 2022 American Chemical Society].

scribed in detail in our previously published work [33], we only briefly describe the overall working of the integrated process in the following.

The compression section consists of two compression stages and supplies compressed air to the cryogenic section. In each compression stage, the air is first compressed (K101 and K102), then cooled in a water-cooled heat exchanger (E101 and E102), and finally passed through a knock-out drum (D101 and D102) to remove any condensed moisture. The leftover moisture and CO_2 are eliminated using an adsorber (A101). Two fractions of the compressed air stream are created with split fractions of 0.32 (S114) and 0.68 (S115).

In the cryogenic section, these two streams of compressed air (S114 and S115) are fed to the 1st multistream heat exchanger (E104) where they are cooled to cryogenic temperatures through heat exchange with the LNG (S402 and S404) and LP column product streams (S127, S129, and S132). The resulting streams (S116 and S117) are then throttled using valves (V101 and V102) and supplied to the HP column (C101) for preliminary separation of air into nitrogen- and oxygen-rich streams. In the 2nd multistream heat exchanger (E105), the top product of the LP column (S126) is used to further cool the top and bottom products from the HP column (S120 and S121). The cooled products (S122 and S123) are then fed to the LP column for final separation, resulting in the production of 99.1 mol% nitrogen (obtained as the top product, S126), and 99.1 mol% oxygen (obtained as the bottom product, S129). Waste streams (S131A and S131B) are withdrawn from the 8th and 46th stages of the LP column to maintain the purity of the products by purging argon from the system.

Imported LNG (CH_4: 0.943352, C_2H_6: 0.041257, C_3H_8: 0.00988, C_4H_{10}: 0.003227, and N_2: 0.002284) is fed to the 1st multistream heat exchanger (E104) at a pressure of 60 bar using the pump P401. The LNG stream (S402) is regasified while its cryogenic energy is utilized to cool the compressed air streams (S114 and S115). The regasified LNG (S403) is used to produce power using a turbine (T401). The resulting LNG expansion causes significant cooling and allows the LNG to be regasified in E104 for a second time. The resulting LNG stream (S405) is mixed with nitrogen (S128B) to reduce the calorific value of the final stream (S406) from 1,062 Btu/scf to 972 BTU/scf (within the required range of 950-1,000 Btu/scf) for onward use in the existing natural gas-based power plants. Table S1 (Supporting Information) presents steady-state simulation results for temperature, pressure, flow rates, and composition for all streams in the integrated process.

The steady-state simulation model developed in this work employs two types of heat exchanger models available in Aspen Plus®: (1) HeatX for water-cooled heat exchangers, and (2) MHeatX for multistream heat exchangers. Detailed zone analysis of both multistream heat exchangers (E104 and E105) was conducted to ascertain the minimum approach temperature (ΔT_{min}). Table S2 (Supporing Information) provides heat duties, minimum approach temperature, and actual LMTD for all exchangers in the integrated process.

Compressors (K101 and K102) and pumps (P201 and P401) require electrical energy for their operation, while the turbine (T401) produces power. The power required (or produced) by this equipment, and the corresponding pressure ratios and assumed efficiencies are reported in Table S3 (Supporting Information).

1. Exergy Analysis

The integrated process is examined using exergy analysis to compute the irreversibilities in the process. An exergy balance is applied to each equipment using the fuel-product technique [53]. The value of exergy efficiency for each equipment is calculated as the ratio of product exergy to fuel exergy. The exergy destruction for each equipment is calculated by subtracting the product exergy from the fuel exergy. The expressions for exergy efficiency and exergy destruction for the various equipment are listed in Table 1. Table S4 (Supporting Information) provides the complete exergy balance equations for each equipment in the integrated process.

2. Exergoeconomic Analysis

Exergoeconomic analysis is useful to provide an efficient design

Table 1. Expressions for exergy efficiency and exergy destruction for various equipment in the integrated process [50,54-58]

Equipment	Exergy destruction $E_{d,k}$, (kW)	Exergy efficiency ε_k, (%)
HP column	$\Sigma E_{in}+\Sigma E_q-\Sigma E_{out}$	$\frac{\Sigma E_{out}}{\Sigma E_{in}+\Sigma E_q}\times 100$
LP column	$\Sigma E_{in}-\Sigma E_{out}-\Sigma E_q$	$\frac{\Sigma E_{out}+\Sigma E_q}{\Sigma E_{in}}\times 100$
Heat exchanger, valve	$\Sigma E_{in}-\Sigma E_{out}$	$\frac{\Sigma E_{out}}{\Sigma E_{in}}\times 100$
Turbine	$\Sigma E_{in}-\Sigma E_{out}-W$	$\frac{W}{\Sigma E_{in}-\Sigma E_{out}}\times 100$
Pump, compressor	$W+\Sigma E_{in}-\Sigma E_{out}$	$\frac{\Sigma E_{out}-\Sigma E_{in}}{W}\times 100$
Exergy destruction ratio (%)	$y_{d,k}=\frac{E_{d,k}}{E_{f,k}}\times 100$	
Overall exergy efficiency (%)	$\frac{E_{out}+W_{out}}{E_{in}+W_{in}}\times 100$	

of a process by combining the principles of exergy (that is, thermodynamics) and economics. This analysis mainly consists of two steps: (1) computing the exergy flows, and (2) computing the cost of all process streams with the help of an economic model [42,59]. The following Eqs. (1)-(4) form the basis of this cost balance:

$$\Sigma_{in}C_{in}+C_q+Z_k=\Sigma_{out}C_{out}+C_w \quad (1)$$

$$C=cE \quad (2)$$

$$C_q=cE_q \quad (3)$$

$$C_w=cW \quad (4)$$

Here, C shows the cost related to the exergy stream, while all the remaining costs are represented by Z_k. The cost per unit of exergy is represented by c, W represents the work produced or consumed by the component, E represents the exergy value of the process stream, and E_q represents the exergy value related to heat transfer. Z_k is computed using Eqs. (5)-(7):

$$Z_k=\frac{\dot{Z}_k\cdot\varphi\cdot CRF}{H} \quad (5)$$

$$\dot{Z}_k=\dot{Z}_k^{CI}+\dot{Z}_k^{OM} \quad (6)$$

$$CRF=\frac{(1+i)^N\cdot i}{(1+i)^N-1} \quad (7)$$

Here, the purchased cost of equipment is represented by $\dot{Z}_k$, the interest rate is represented by i, plant lifetime is represented by N, maintenance factor is represented by φ, capital recovery factor is represented by CRF, and H represents the annual plant working hours. Table 2 summarizes the assumptions used in the current work for performing the exergoeconomic analysis. The equations used to compute the purchased cost for individual equipment are listed in Table 3.

Usually, there is only one unknown variable while solving exergoeconomic equations across a given component. Additional equations are required when more than one unknown is involved. Such auxiliary equations can be developed using the fuel-product concept for the exergy streams [53]. In a control volume, the product characterizes the required results produced by using the fuel, while the fuel characterizes the source of exergy required for product generation. The concept of "fuel" in the context of exergoeconomic analysis is different from the commonly understood fuels, i.e., coal, oil, natural gas, etc.

Table 2. Assumptions for the exergoeconomic analysis [50,60,61]

Assumptions	Value
Isentropic efficiency of compressors/turbine (%)	72.0
Isentropic efficiency of pumps (%)	80.0
Maintenance factor	1.06
Interest rate (%)	8.0
Plant lifetime (years)	20
Cost per exergy unit of electricity ($/GJ) [62]	25.00
Cost per exergy unit of LNG ($/GJ) [27]	13.69
Plant annual working hours (H)	8,000

Table 4 lists the cost balance equations as well as the auxiliary equations (where required) for all equipment in the integrated process.

For process equipment k as a control volume, the product and fuel costs per unit exergy are calculated using Eqs. (8)-(9):

$$c_{p,k}=\frac{C_{p,k}}{E_{p,k}} \quad (8)$$

$$c_{f,k}=\frac{C_{f,k}}{E_{f,k}} \quad (9)$$

The amount of wasted money associated with the operation of a component is represented by the exergy destruction cost rate ($C_{d,k}$) It identifies process components that are responsible for most exergoeconomic loss and provides a systematic mechanism to improve the process.

$$C_{d,k}=E_{d,k}\cdot c_{f,k} \quad (10)$$

The relative cost difference (r_k) accounts for the investment and exergy destruction costs and is computed by the difference between

Table 3. Equations for the cost analysis of various components

Equipment	Equations for cost analysis
Flash drum [63]	$PEC=F_m\cdot C_b+C_a$ $C_a=480\cdot D^{0.7396}\cdot L^{0.7066}$ $C_b=1.672\cdot\exp[9.1-0.2889(\ln W)+0.04576(\ln W)^2]$
Compressors [63]	$PEC=F_D\cdot F_M\cdot C_B$ $C_B=\exp[9.1553+0.63\ln(P_c)]$
Tower [64]	$PEC=F_m\cdot C_V+C_{PL}+C_T$ $C_{PL}=341\cdot D^{0.63316}\cdot L^{0.80161}$ $C_V=\exp[10.5449-0.4672(\ln W)+0.05482(\ln W)^2]$ $C_T=468\cdot n\cdot(1.189+0.0577D)\cdot\exp(0.1482D)$
MHEX [32,65]	$PEC=130\cdot\left(\frac{A}{0.093}\right)^{0.78}$
Pump [66]	$\log_{10}(PEC)=3.3892+0.0536\log_{10}(P_c)+0.1538[\log_{10}(P_c)]^2$
Heat exchangers [66]	$\log_{10}(PEC)=4.3247-0.3030\log_{10}(A)+0.1634[\log_{10}(A)]^2$
Turbine [66]	$\log_{10}(PEC)=2.2476+1.4965\log_{10}(P_c)-0.1618[\log_{10}(P_c)]^2$

Table 4. Cost balance and auxiliary equations for equipment in the integrated process

Equipment	Cost balance	Auxiliary equation
K101	$C_{S101}+C_W+Z_{K101}=C_{S102}$	$c_{S101}=0$
K102	$C_{S104}+C_W+Z_{K102}=C_{S105}$	None
E101	$C_{S102}+C_{W203A}+Z_{E101}=C_{S103}+C_{W204}$	$c_{W203A}=c_{W204}$
E102	$C_{S105}+C_{W203B}+Z_{E102}=C_{S106}+C_{W205}$	$c_{W203B}=c_{W205}$
D101	$C_{S103}+Z_{D101}=C_{S104}+C_{PRG1}$	$c_{S104}=c_{PRG1}$
D102	$C_{S106}+Z_{D102}=C_{S107}+C_{PRG2}$	$c_{S107}=c_{PRG2}$
A101	$C_{S107}+Z_{A101}=C_{S111}+C_{PRG3}$	$c_{S111}=c_{PRG3}$
F101	$C_{S111}=C_{S114}+C_{S115}$	$c_{S114}=c_{S115}$
F201	$C_{W202}=C_{W203A}+C_{W203B}$	$c_{W203A}=c_{W203B}$
P201	$C_{W201}+C_W+Z_{P201}=C_{W202}$	$c_{W201}=0$
P401	$C_{S401}+C_W+Z_{P401}=C_{S402}$	None
E104	$C_{S114}+C_{S115}+C_{S127}+C_{S129}+C_{S132}+C_{S402}+C_{S404}+Z_{E104}=C_{S116}+C_{S117}+C_{S128}+C_{S130}+C_{S133}+C_{S403}+C_{S405}$	$\frac{C_{S116}-C_{S114}}{E_{S116}-E_{S114}}=\frac{C_{S117}-C_{S115}}{E_{S117}-E_{S115}}$, $c_{S127}=c_{S128}$, $c_{S129}=c_{S130}$, $c_{S132}=c_{S133}$, $c_{S402}=c_{S403}$, $c_{S404}=c_{S405}$
E105	$C_{S120}+C_{S121}+C_{S126}+Z_{E105}=C_{S122}+C_{S123}+C_{S127}$	$\frac{C_{S122}-C_{S120}}{E_{S122}-E_{S120}}=\frac{C_{S123}-C_{S121}}{E_{S123}-E_{S121}}$, $c_{S126}=c_{S127}$
C101	$C_{S118}+C_{S119}+Z_{C101}=C_{S120}+C_{S121}$	$c_{S120}=c_{S121}$
C102	$C_{S124}+C_{S125}+Z_{C102}=C_{S126}+C_{S129}+C_{S131A}+C_{S131B}$	$c_{S126}=c_{S129}$, $c_{S129}=c_{S131A}$, $c_{S131A}=c_{S131B}$
T401	$C_{S403}+Z_{T401}=C_{S404}+C_W$	None
V101	$C_{S116}=C_{S118}$	None
V102	$C_{S117}=C_{S119}$	None
V103	$C_{S122}=C_{S124}$	None
V104	$C_{S123}=C_{S125}$	None
F401	$C_{S128}=C_{S128A}+C_{S128B}$	$c_{S128A}=c_{S128B}$
M101	$C_{S131A}+C_{S131B}=C_{S132}$	None
M401	$C_{S405}+C_{S128B}=C_{S406}$	None

the average product cost and the average fuel cost:

$$r_k(\%)=\frac{c_{p,k}-c_{f,k}}{c_{f,k}}\times 100 \quad (11)$$

The exergoeconomic factor (f_k) is the most significant outcome of exergoeconomic analysis. A high value of the exergoeconomic factor represents a high share of investment cost and a low share of exergy destruction, whereas a low value of this factor reflects a high share of exergy destruction and a low share of investment cost [50,60,61,67-69].

$$f_k(\%)=\frac{Z_k}{Z_k+C_{d,k}}\times 100 \quad (12)$$

RESULTS AND DISCUSSION

1. Exergy and Cost Values

The exergy and cost analyses of each process stream are demonstrated in Table 5. The exergy values are computed based on a reference pressure of 1.01325 bar and a reference temperature of 25 °C. The cost values are calculated during the exergoeconomic analysis as described above. It should be emphasized that for meaningful interpretation of these data, both the exergy flow (kW) and the cost per unit exergy ($/GJ) should be simultaneously considered. For example, the highest values of exergy flow are observed for the cooling water streams. However, this is due to their large flow rate rather than their departure from the reference conditions. As a result, the cost per unit exergy for these streams is negligible (0.01 $/GJ) and they have little impact on the overall cost flow (6-14 $/h). On the other hand, high-purity oxygen and nitrogen streams have the highest cost per unit exergy (118-122 $/GJ) due to significant departure from the reference conditions and also the highest cost flow (8,000-12,500 $/h).

2. Exergy Analysis

Exergy analysis involves the calculation of both exergy efficiency (%) and exergy destruction (kW). Fig. 2 presents the exergy efficiencies (%) of all equipment in the integrated process. The analysis shows that the HP column and valves have the highest exergy efficiency (>99%), followed by the water pump, water-cooled and multistream heat exchangers, compressors, turbine, and LNG pump. We note here that the exergy efficiency of the LP column is lower than the HP column. This is because the HP column produces only partial separation between oxygen and nitrogen and hence causes lower exergy destruction. On the other hand, the LP column produces sharp separation between oxygen and nitrogen which results in higher exergy destruction. Similarly, the exergy efficiencies of the multistream heat exchangers are higher than the exergy efficiencies of the water-cooled heat exchangers. This is because the multistream

Table 5. Exergy and cost values of the process streams

Stream #	E_{tot} (kW)	C ($/h)	c ($/GJ)
S101	248.08	0.00	0.00
S102	14,513.48	1,683.97	32.23
S103	11,058.72	1,685.22	42.33
S104	11,058.72	1,690.79	42.47
S105	25,878.51	3,424.66	36.76
S106	21,990.52	3,427.09	43.29
S107	21,973.74	3,377.01	42.69
S111	21,992.04	3,325.20	42.00
S114	7,037.45	1,064.06	42.00
S115	14,954.58	2,261.13	42.00
S116	25,380.52	9,904.50	108.40
S117	27,389.59	8,255.99	83.73
S118	25,369.33	9,909.26	108.50
S119	27,277.71	8,255.65	84.07
S120	36,482.78	7,373.32	56.14
S121	53,415.36	10,795.46	56.14
S122	37,621.37	8,001.61	59.08
S123	56,481.46	12,488.73	61.42
S124	37,266.93	8,001.36	59.64
S125	56,160.24	12,488.47	61.77
S126	23,911.48	10,209.25	118.60
S127	18,493.27	7,895.89	118.60
S128	3,209.63	1,370.38	118.60
S128A	3,201.92	1,367.09	118.60
S128B	7.71	3.29	118.60
S129	21,971.01	9,380.74	118.60
S130	4,744.06	2,025.52	118.60
S131A	1,056.18	450.95	118.60
S131B	1,159.95	495.25	118.60
S132	2,138.89	945.56	122.80
S133	182.54	80.70	122.80
S401	87,257.66	4,300.41	13.69
S402	87,264.14	4,303.87	13.70
S403	86,518.86	4,267.11	13.70
S404	85,809.58	4,232.13	13.70
S405	85,584.95	4,221.05	13.70
S406	85,519.38	4,223.97	13.72
PRG1	0.00	0.00	42.47
PRG2	358.29	55.06	42.69
PRG3	377.61	57.09	42.00
W201	287,086.98	0.00	0.00
W202	287,233.55	14.11	0.01
W203A	129,041.00	6.34	0.01
W203B	158,192.46	7.77	0.01
W204	129,442.44	6.36	0.01
W205	158,684.60	7.80	0.01

heat exchangers operate with minimal temperature difference driving force and therefore cause minimal irreversibility in the heat transfer process. On the other hand, water-cooled heat exchangers operate with finite temperature difference driving force which results in higher exergy destruction.

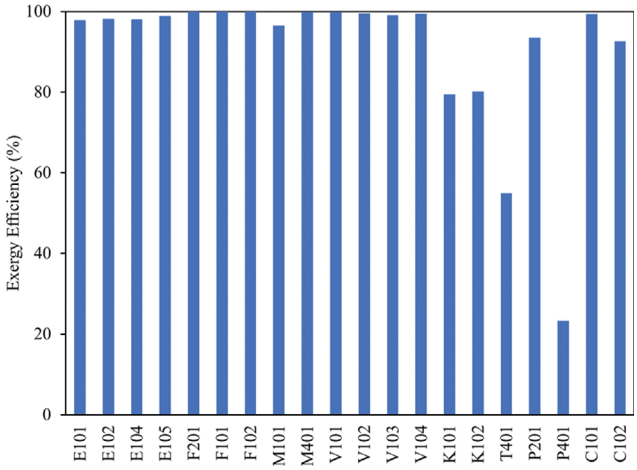

Fig. 2. Percent exergy efficiency of equipment in the integrated process.

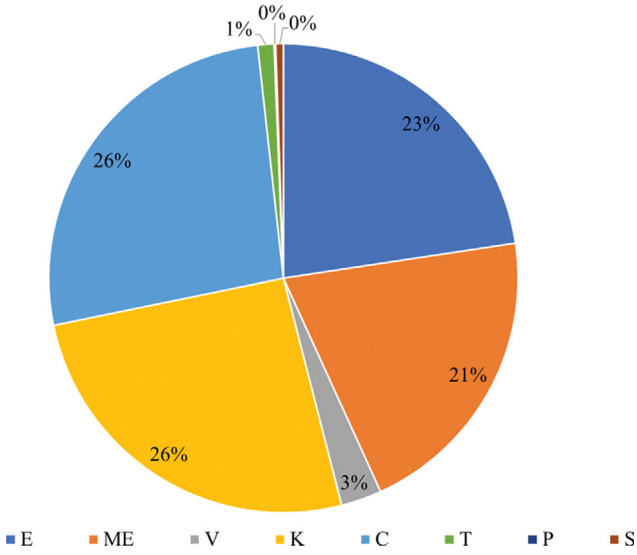

Fig. 3. Percent contribution of individual equipment toward total exergy destruction in the integrated process (C: column, ME: multistream heat exchangers, E: water-cooled heat exchangers, V: valves, K: compressors, T: turbine, P: pumps, S: flash separators and adsorbers).

The integrated process has an overall exergy efficiency of 76.47% and a total exergy destruction rate of 28.52 MW. Fig. 3 shows the % contribution of different process equipment toward the total exergy destruction in the integrated process. The analysis shows that the compression section (including the compressors and the water-cooled heat exchangers) causes major exergy destruction in the process (48%), followed by the distillation columns (26%) and the multistream heat exchangers (21%). The electrical energy used to drive the compressors is ultimately converted to thermal energy and raises the temperature of the air being compressed. When this compressed air is cooled in water-cooled heat exchangers, the energy is inevitably lost to the environment. This process is inherently irreversible and a source of major exergy destruction in the process. The

Table 6. Outcomes of process exergy and exergoeconomic analyses

Equipment	$E_{f,k}$ (MW)	$E_{p,k}$ (MW)	$E_{d,k}$ (MW)	$c_{f,k}$ ($/GJ)	$c_{p,k}$ ($/GJ)	$C_{d,k}$ ($/h)	Z_k ($/h)	ε_k (%)	$y_{d,k}$ (%)	r_k (%)	f_k (%)
K101	18.19	14.51	3.68	25.00	32.82	331.09	70.33	79.50	20.22	31.28	17.52
K102	29.55	25.88	3.67	25.00	32.54	330.39	71.68	80.15	12.42	30.16	17.83
E101	143.55	140.50	3.05	3.27	3.35	35.99	1.59	97.87	2.13	2.25	4.24
E102	184.07	180.68	3.40	5.18	5.28	63.35	1.92	98.16	1.84	1.92	2.94
P201	287.24	287.23	0.01	25.00	28.14	0.91	0.75	93.52	0.00	12.56	44.92
E104	237.67	233.01	4.66	35.23	35.98	590.89	38.90	98.04	1.96	2.12	6.18
E105	113.81	112.60	1.21	69.47	70.24	303.51	6.83	98.93	1.07	1.10	2.20
T401	86.52	86.20	0.32	12.49	25.00	14.37	3.52	54.95	0.37	100.16	19.70
C101	90.53	89.90	0.63	39.61	60.65	90.08	22.61	99.30	0.70	53.13	20.06
C102	93.43	86.51	6.91	61.09	66.16	1,520.69	49.77	92.60	7.40	8.29	3.17
P401	87.29	87.26	0.02	25.00	148.25	1.91	0.56	23.37	0.02	493.00	22.52

remaining equipment has negligible contribution toward exergy destruction in the process.

It should be emphasized that for meaningful interpretation of the results of exergy analysis, both exergy destruction (kW) and exergy efficiency (%) should be simultaneously considered. For example, the LNG pump (P401) has an exergy efficiency of only 21%. However, its contribution toward total exergy destruction in the process is less than 0.1%, implying that this pump is insignificant in the larger picture. The LP column (C102), on the other hand, is responsible for 24.2% of the overall exergy degradation in the process, even though its exergy efficiency is reasonably high (92.6%).

3. Exergoeconomic Analysis

In the exergoeconomic analysis, a cost balance is written for each equipment. The resulting set of equations is simultaneously solved to calculate the costs associated with each process stream. The results of this exergoeconomic analysis are presented in Table 6. The exergoeconomic factor (f_k) gives valuable information regarding the balance of investment and exergy destruction costs. A low value of the exergoeconomic factor represents a situation where the exergy destruction costs are more important than the capital investment (CI) and operating and maintenance (O&M) costs. In this case, the focus should be on improving the performance of the equipment. On the other hand, if the value of f_k is high, the contribution of CI and O&M costs will be more significant than the contribution of exergy destruction caused by the equipment. In this case, minimizing the cost of the equipment should be the prime objective.

Results of the exergoeconomic analysis (Table 6) reveal that the value of f_k is comparatively high for pumps P201 and P401, HP column C101, turbine T401, and compressors K101 and K102. Therefore, the emphasis should be on lowering the cost of this equipment to decrease the total cost of the system. The value of f_k is low for the 2nd multistream heat exchanger E105, 2nd water-cooled heat exchanger E102, and the LP column C102. For this equipment, the focus should be on improving the equipment efficiency.

The relative cost difference (r_k) is a measure of the increase in the product's exergy cost relative to the fuel's exergy cost. Its numerical value represents the significance of a given piece of equipment for the optimization of the overall process. Table 6 shows that the highest r_k values are observed for the LNG pump P401 and the turbine T401. However, because the corresponding exergy destruction cost is small, i.e., 1.91 $/h for P401 and 14.37 $/h for T401, they are insignificant in the larger picture. The lowest value of r_k is ob-

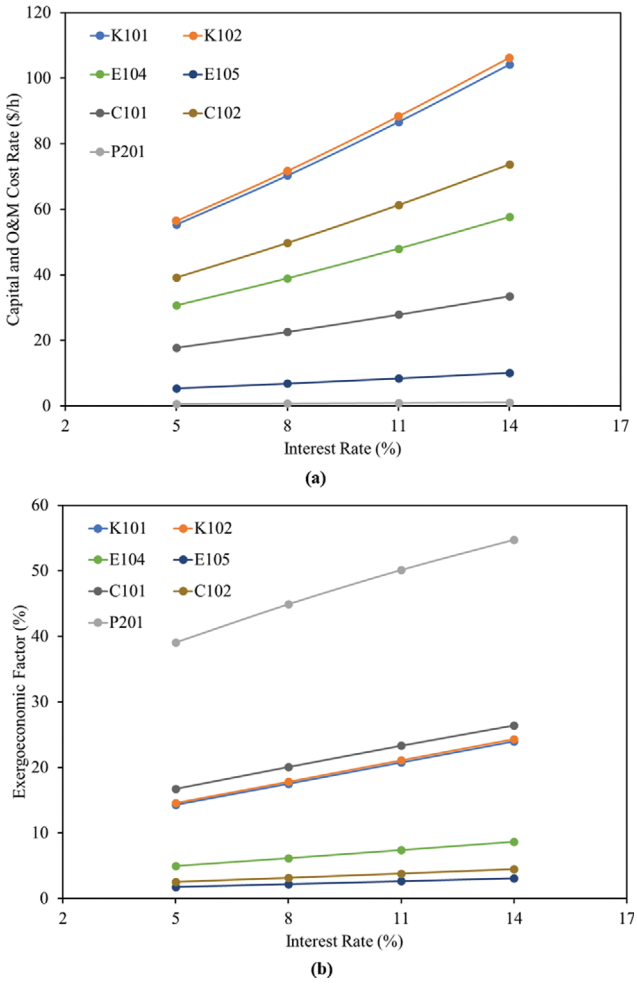

Fig. 4. Effect of interest rate (%) on the (a) cost rate ($/h), and (b) exergoeconomic factor (%).

served for the 2nd multistream heat exchanger E105. The current performance of the process equipment is represented by the exergy destruction cost rate $C_{d,k}$. The highest value of this factor is observed for the LP column C102, and the lowest value is observed for the cooling water pump P201.

4. Parametric Study

Process optimization is a key objective for the best possible operation of a facility/plant. Parametric studies play an important role for process optimization by describing the effect of key parameters on the objective function and thus choosing their optimal values. Fig. 4 represents the impact of the interest rate (%) on the (a) CI and O&M costs ($/h), and (b) exergoeconomic factor (%) of the major components. In this case, the plant operational hours (8,000 hours/year) and plant lifetime (20 years) are kept constant.

The sensitivity analysis reveals that with a rise in the interest rate from 5 to 14%, the impact on the cost of the air compressors (K101 and K102) is significant. Table 6 shows that these compressors have the highest investment cost rate (70.33 and 71.68 $/h, respectively). Because of their higher contribution to the total cost rate of the process, an increase in the interest rate has a pronounced impact on the corresponding capital and O&M cost rates (as indicated by steeper curves in Fig. 4). On the hand, the cost rates of the columns (C101: 22.61 $/h and C102: 49.77 $/h) and the multistream heat exchangers (E104: 38.90 $/h and E105: 6.83 $/h) are significantly lower. As a result, the effect of increase in interest rate on the capital and O&M cost rates of these equipment is less pronounced (as indicated by moderately sloped curves in Fig. 4).

In the case of the exergoeconomic factor, the largest effect is observed in the case of the water pump P201, followed by the HP column C101, and compressors K102 and K101, while the least effect is observed in the case of E105 and C102. We conclude that the larger the value of the exergoeconomic factor for an equipment, the more sensitive it is to changes in interest rate.

Although the effect of interest rate is not significant on the cost of pump P201, the increase in cost has led to a significant increase in the value of exergoeconomic factor, because the exergy destruction rate is very small (156.73 kW, less than 0.1% of the overall exergy destruction rate). The same is true for all equipment, on which varying interest rates produced a significant effect on their cost and eventually the exergoeconomic factor.

The effect of plant lifetime (years) on the (a) cost rate ($/h) and (b) exergoeconomic factor (%) is presented in Fig. 5. The plant lifetime is varied from 5 to 25 years, with a step size of 5 years, while interest rate (8%) and the number of operational hours (8,000 hours/year) are kept constant. The analysis shows that with an increase in plant lifetime, both the cost rate and the exergoeconomic factor decrease. This trend appears because plant lifetime is inversely proportional to these factors. Likewise, during the variation of the interest rate (%), the effect of plant life on the cost of compressors K102 and K101 is higher, with the effect on other components being comparatively small. Similarly, the variation of plant lifetime on exergoeconomic factors of P201 and C101 is higher, as in the case of interest rate, while there is minimal effect on the exergoeconomic factors of E105 and C102. Moreover, the trend shows that while increasing the plant lifetime from 5 to 10 years, the difference is significant, while from 10 to 25 years, the difference is comparatively smaller. This can be explained by the change in the value of the capital recovery factor (CRF). For plant lifetimes of 5, 10, 15, 20, and 25 years, the CRF is 0.2505, 0.1490, 0.1168, 0.1019, and 0.0937, respectively. Clearly, the decrease in CRF is initially rapid but gradually slows down for plant lifetimes exceeding 15 years. However, as plant life is linked with various direct and indirect costs, a large lifetime of the plant (usually 15-20 years) is required.

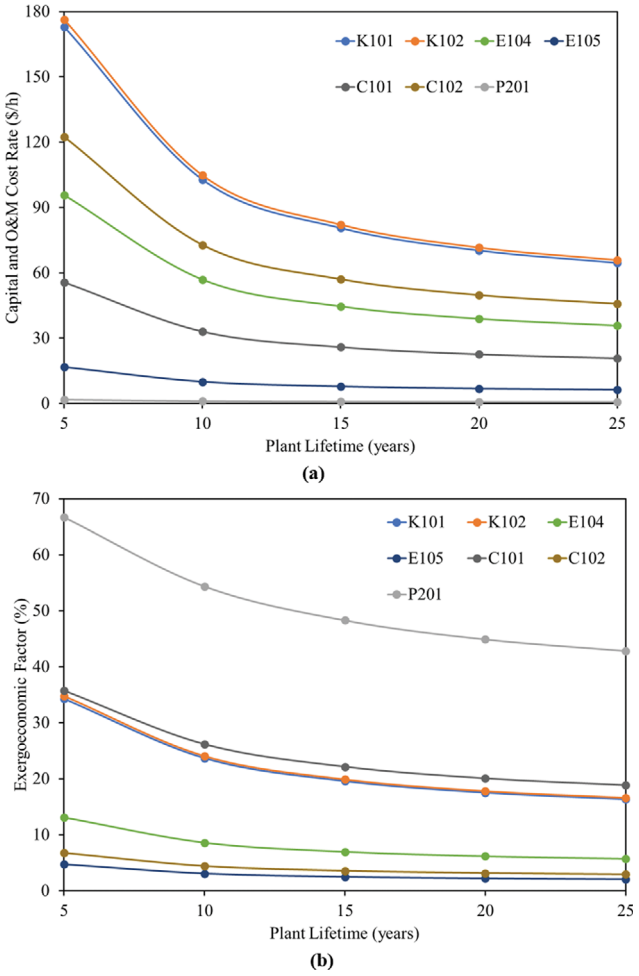

Fig. 5. Effect of plant lifetime on (a) cost rate ($/h), and (b) exergoeconomic factor (%).

Fig. 6 shows the impact of the isentropic efficiency (%) of the compressor K101 on (a) exergy efficiency (%) and exergoeconomic factor, and (b) exergy destruction cost rate and CI and O&M cost rates ($/h). The analysis demonstrates that the values of exergy efficiency (%) and exergoeconomic factor (%) increase almost linearly when the isentropic efficiency of the compressor K101 is increased from 72% to 84%. When exergy efficiency (%) increases, the power consumption of the compressor (kW) decreases. As a result, the exergy destruction, CI and O&M cost rates decrease.

An increase in the isentropic efficiency of the compressor K102 would produce the same pattern. Because the exergoeconomic factor is increasing, it can be concluded that compressor efficiency has a bigger influence on reducing exergy destruction (kW) and associated cost rates ($/h) than lowering CI and O&M prices. Therefore, an efficient design is required to reduce the CI & OM costs

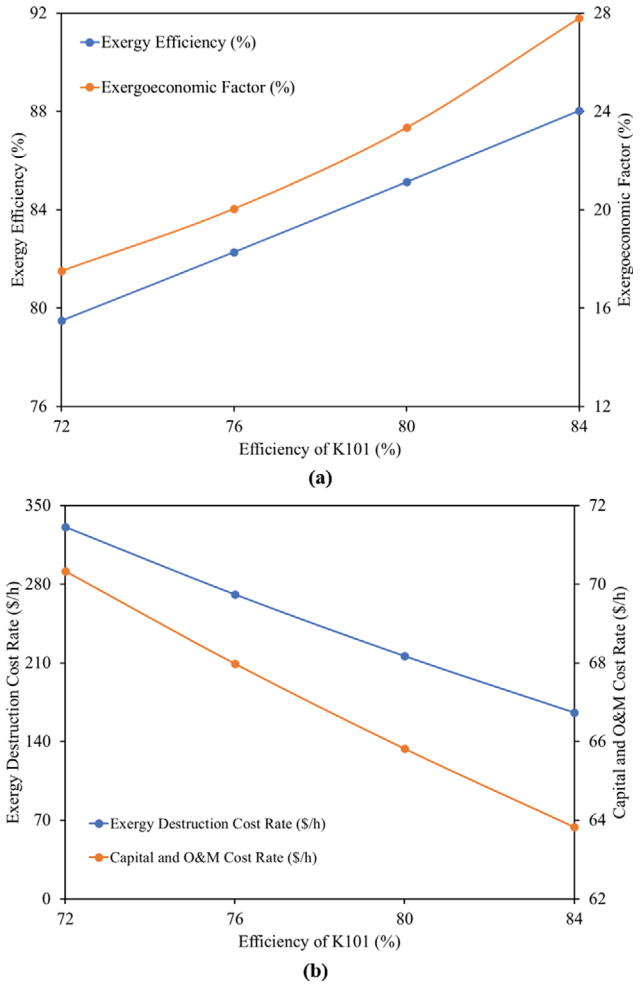

Fig. 6. Effect of isentropic efficiency of compressor K101 on (a) exergy efficiency and exergoeconomic factor, (b) exergy destruction cost rate and capital investment (CI) and operating and maintenance (O&M) cost rate.

which would eventually lead to improved performance of the compressor and the overall system.

CONCLUSIONS

An integrated LNG regasification - air separation process was evaluated using exergy and exergoeconomic analyses. Exergy destruction cost rates, as well as cost rates due to capital investment (CI) and operation and maintenance (O&M) of various components were calculated. The results were used to identify the weakest process components and the opportunities for improvement using parametric studies.

- The compression section is responsible for significant exergy destruction (48%) in the process and should be given priority for modification/improvement. The next higher contributors to exergy destruction are distillation columns (26%) and multistream heat exchangers (21%).
- The highest exergy destruction cost rates are observed for the LP column and the 1st multistream heat exchanger (1,520.7 and 590.9 $/h, respectively), while the lowest exergy destruction cost rates are associated with the water and LNG pumps (0.9 $/h for P201 and 1.9 $/h for P401).
- The highest values of exergoeconomic factors are associated with the water and LNG pumps (44.92% and 22.52%, respectively), indicating that the cost of these components should be reduced. However, the resulting gain will be minimal because these pumps account for only 0.1% of the total exergy destruction in the process.
- A parametric study revealed that the interest rate is in a direct relationship and the number of years of plant life is in an indirect relationship with the exergoeconomic factor. Furthermore, the compressors are causing significant exergy destruction and have higher values of exergoeconomic factor, indicating that a more efficient design is needed to improve the overall system performance.

ACKNOWLEDGEMENT

The authors gratefully acknowledge the financial support of the SNGPL Chair of Gas Engineering in the Department of Chemical Engineering, University of Engineering & Technology, Lahore.

NOMENCLATURE

A : area [m^2]
C : cost rate [$/h]
$C_{d,k}$: exergy destruction cost rate for equipment k [$/h]
$C_{f,k}$: exergy destruction cost rate for an inlet stream to equipment k [$/h]
$C_{p,k}$: exergy destruction cost rate for an outlet stream from equipment k [$/h]
c : cost per unit exergy [$/GJ]
$c_{f,k}$: cost per unit exergy for an inlet stream to equipment k [$/GJ]
$c_{p,k}$: cost per unit exergy for an outlet stream from equipment k [$/GJ]
D : diameter of the vessel [m]
E : exergy of a stream
E_{chem} : chemical exergy of a stream [kW]
E_{phy} : physical exergy of a stream [kW]
E_{tot} : total exergy of a stream [kW]
E_{in} : exergy of an inlet stream [kW]
E_{out} : exergy of an outlet stream [kW]
$E_{d,k}$: exergy destruction in equipment k [kW]
$E_{f,k}$: exergy of an inlet stream to equipment k [kW]
$E_{p,k}$: exergy of an outlet stream from equipment k [kW]
E_q : exergy corresponding to heat flow (kW)$=Q\left(\frac{T_0}{T}-1\right)$
f_k : exergoeconomic factor [%]
F : flow rate [TPH, tons per hour]
F_D : driver (electric motor, steam turbine, etc.) factor
F_M : material factor
H : annual working hours [h]
i : interest rate [%]
L : length/tangent to tangent height of the vessel [m]

N : plant lifetime [years]
n : number of trays
PEC : purchased equipment cost [$]
P_o : reference pressure [1.01325 bar]
P_c : power [kW]
Q : heat flow [kW]
r_k : relative cost difference [%]
ΔT_{min} : minimum approach temperature [K]
T_o : reference temperature [298.15 K]
W : mechanical work [kW]
W_p : work required by the pump [kW]
W_{in} : work required (for pumps and compressors) [kW]
W_{out} : work produced (from turbine) [kW]
$y_{D,k}$: exergy destruction ratio [%]
Z_k : investment cost rate [$/h]

Greek Letters

ε_k : exergy efficiency [%]
η_p : pump efficiency [%]

Subscript

f : feed
p : product
k : k-th equipment

Abbreviations

ASU : air separation unit
CI : capital investment
EES : engineering equation solver
HP : horsepower
LNG : liquefied natural gas
LMTD : log mean temperature difference
O&M : operations and maintenance
TPH : tons per hour

DECLARATION OF COMPETING INTEREST

The authors declare that they have no known competing financial interests or personal relationships that could have appeared to influence the work reported in this paper.

SUPPORTING INFORMATION

Additional information as noted in the text. This information is available via the Internet at http://www.springer.com/chemistry/journal/11814.

REFERENCES

1. A. Atienza-Márquez, J. C. Bruno and A. Coronas, *Appl. Therm. Eng.*, **132**, 463 (2018).
2. J. Pospíšil, P. Charvát, O. Arsenyeva, L. Klimeš, M. Špiláček and J. J. Klemeš, *Renew. Sust. Energy Rev.*, **99**, 1 (2019).
3. A. Mahmood, N. Javaid, A. Zafar, R. A. Riaz, S. Ahmed and S. Razzaq, *Renew. Sust. Energy Rev.*, **31**, 182 (2014).
4. K. Bakht, F. Aslam, T. Nawaz and B. Seerat, *Int. J. Adv. Comput. Sci. Appl.*, **7**, 66 (2016).
5. Exxon Mobil Corporation, *2019 Outlook for Energy: A Perspective to 2040* (2019).
6. U. Perwez, A. Sohail, S. F. Hassan and U. Zia, *Energy*, **93**, 2423 (2015).
7. S. Malik, M. Qasim, H. Saeed, Y. Chang and F. Taghizadeh-Hesary, *Energy Policy*, **144**, 111552 (2020).
8. Ministry of Planning Development & Special Initiatives (Government of Pakistan), *Pakistan Natural Gas: Policy Analysis & Way Forward*, Islamabad, Pakistan (2023).
9. British Petroleum, *BP Statistical Review of World Energy 2021* (2021).
10. National Electric Power Regulatory Authority (NEPRA), *State of Industry Report 2022*, Islamabad, Pakistan (2022).
11. P. Dorosz, P. Wojcieszak and Z. Malecha, *Entropy*, **20**, 59 (2018).
12. D. Fioriti, A. Baccioli, G. Pasini, A. Bischi, F. Migliarini, D. Poli and L. Ferrari, *Energy Convers. Manage.*, **238**, 114128 (2021).
13. I. Szczygiel and Z. Bulinski, *Energy*, **165**, 999 (2018).
14. J. Bao, T. Yuan, L. Zhang, N. Zhang, X. Zhang and G. He, *Energy Convers. Manage.*, **184**, 107 (2019).
15. M. Mehrpooya, M. Kalhorzadeh and M. Chahartaghi, *J. Cleaner Prod.*, **113**, 411 (2016).
16. A. Ebrahimi and M. Ziabasharhagh, *Energy*, **126**, 868 (2017).
17. D. Kim, R. E. H. Giametta and T. Gundersen, *Ind. Eng. Chem. Res.*, **57**, 5914 (2018).
18. T. Gao, W. Lin and A. Gu, *Energy Convers. Manage.*, **52**, 2401 (2011).
19. G. Tsatsaronis and T. Morosuk, *Energy*, **35**, 820 (2010).
20. M. Mehrpooya, R. Esfilar and S. M. A. Moosavian, *J. Cleaner Prod.*, **142**, 1749 (2017).
21. S. Chen, J. Xu, X. Dong, H. Zhang, Q. Gao and C. Tan, *Int. J. Refrig.*, **90**, 264 (2018).
22. H. Dhameliya and P. Agrawal, *Energy Procedia*, **90**, 660 (2016).
23. P. Wang and T.-S. Chung, *Water Res.*, **46**, 4037 (2012).
24. C. Dispenza, G. Dispenza, V. La Rocca and G. Panno, *Appl. Therm. Eng.*, **29**, 3595 (2009).
25. I. Lee, J. Park and I. Moon, *Energy*, **140**, 106 (2017).
26. Confidential, Design specification of a gas-fired power plant in Pakistan (n.d.).
27. M. Mehrpooya and H. Ansarinasab, *Energy Convers. Manage.*, **99**, 400 (2015).
28. S. Kumar, H.-T. Kwon, K.-H. Choi, W. Lim, J. H. Cho, K. Tak and I. Moon, *Appl. Energy*, **88**, 4264 (2011).
29. Y. Xiong and B. Hua, *Adv. Mater. Res.*, **881-883**, 653 (2014).
30. T. He, Z. R. Chong, J. Zheng, Y. Ju and P. Linga, *Energy*, **170**, 557 (2019).
31. S. Wang, K. Huang, X. Wang, N. Liao, W. Yan, Q. Pei and B. Xia, *Open Pet. Eng. J.*, **9**, 226 (2016).
32. A. Ebrahimi, M. Meratizaman, H. A. Reyhani, O. Pourali and M. Amidpour, *Energy*, **90**, 1298 (2015).
33. M. H. Hamayun, N. Ramzan, M. Hussain and M. Faheem, *Ind. Eng. Chem. Res.*, **61**, 2843 (2022).
34. Q. Fu, Y. Kansha, C. Song, Y. Liu, M. Ishizuka and A. Tsutsumi, *Appl. Energy*, **162**, 1114 (2016).
35. M. Elhelw, A. A. Alsanousie and A. Attia, *Alexandria Eng. J.*, **59**, 613 (2020).
36. S. Chen, X. Dong, J. Xu, H. Zhang, Q. Gao and C. Tan, *Energy*,

171, 341 (2019).
37. M. Mehrpooya, H. Dehghani and S. M. A. Moosavian, *J. Power Sources*, **306**, 107 (2016).
38. H. Ansarinasab and M. Mehrpooya, *Appl. Therm. Eng.*, **115**, 885 (2017).
39. A. Mohammadi and M. Mehrpooya, *Appl. Therm. Eng.*, **116**, 685 (2017).
40. M. J. Zonouz and M. Mehrpooya, *Energy*, **140**, 261 (2017).
41. H. Ansarinasab, M. Mehrpooya and A. Mohammadi, *J. Cleaner Prod.*, **144**, 248 (2017).
42. M. Mehrpooya, H. Ansarinasab, M. M. M. Sharifzadeh and M. A. Rosen, *Energy Convers. Manage.*, **163**, 151 (2018).
43. W. Xu, J. Duan and W. Mao, *J. Therm. Sci.*, **23**, 77 (2014).
44. T. Morosuk, M. Schult and G. Tsatsaronis, in *ASME 2014 8th International Conference on Energy Sustainability*, ASME, Boston, Massachusetts, USA, p. V002T12A010 (2014).
45. Z. Jieyu, L. Yanzhong, L. Guangpeng and S. Biao, *Phys. Procedia*, **67**, 116 (2015).
46. M. Mehrpooya, M. M. M. Sharifzadeh and M. A. Rosen, *Energy*, **90**, 2047 (2015).
47. R. Esfilar, M. Mehrpooya and S. M. A. Moosavian, *Energy Convers. Manage.*, **157**, 438 (2018).
48. M. Mehrpooya and H. Ansarinasab, *J. Nat. Gas Sci. Eng.*, **26**, 782 (2015).
49. B. Ghorbani, M.-H. Hamedi, R. Shirmohammadi, M. Hamedi and M. Mehrpooya, *Sust. Energy Technol. Assess.*, **17**, 56 (2016).
50. M. Mehrpooya and M. J. Zonouz, *Energy Convers. Manage.*, **139**, 245 (2017).
51. M. Mehrpooya, H. Ansarinasab, M. M. M. Sharifzadeh and M. A. Rosen, *J. Power Sources*, **364**, 299 (2017).
52. Aspentech, Aspen plus is a proprietary software product of Aspentech, https://www.Aspentech.Com.
53. T. J. Kotas, *The exergy method of thermal plant analysis*, Elsevier (1985).
54. S. Tesch, T. Morosuk and G. Tsatsaronis, *Energy*, **141**, 2458 (2017).
55. A. Palizdar, T. Ramezani, Z. Nargessi, S. AmirAfshar, M. Abbasi and A. Vatani, *Energy Convers. Manage.*, **150**, 637 (2017).
56. M. H. Hamayun, N. Ramzan, M. Hussain and M. Faheem, *Energies*, **13**, 6361 (2020).
57. F. Asif, M. H. Hamayun, M. Hussain, A. Hussain, I. M. Maafa and Y.-K. Park, *Sustainability*, **13**, 6490 (2021).
58. M. H. Hamayun, M. Hussain, I. Shafiq, A. Ahmed and Y.-K. Park, *Environ. Eng. Res.*, **27**, 200683 (2022).
59. B. B. Kanbur, L. Xiang, S. Dubey, F. H. Choo and F. Duan, *Renew. Sust. Energy Rev.*, **79**, 1171 (2017).
60. V. M. Ambriz-Díaz, C. Rubio-Maya, E. Ruiz-Casanova, J. Martínez-Patiño and E. Pastor-Martínez, *Energy Convers. Manage.*, **203**, 112227 (2020).
61. C. J. Okereke, O. Lasode and I. O. Ohijeagbon, *Heliyon*, **6**, e04402 (2020).
62. H. Ozcan and I. Dincer, *Int. J. Hydrogen Energy*, **42**, 2435 (2017).
63. J. R. Couper, W. R. Penney, J. R. Fair and S. M. Walas, *Chemical process equipment: Selection and design*, 3rd ed., Elsevier (2012).
64. W. D. Seider, D. R. Lewin, J. D. Seader, S. Widagdo, R. Gani and K. M. Ng, *Product and process design principles: Synthesis, analysis, and evaluation*, 4th ed., John Wiley & Sons, Inc. (2017).
65. V. Eveloy, W. Karunkeyoon, P. Rodgers and A. Al-Alili, *Int. J. Hydrogen Energy*, **41**, 13843 (2016).
66. R. Turton, R. C. Bailie, W. B. Whiting, J. A. Shaeiwitz and D. Bhattacharyya, *Analysis, synthesis, and design of chemical processes*, 4th ed., Prentice Hall (2012).
67. G. Tsatsaronis, *Int. J. Exergy*, **5**, 489 (2008).
68. M. Ameri, P. Ahmadi and A. Hamidi, *Int. J. Energy Res.*, **33**, 499 (2009).
69. C. Uysal, *Environ. Prog. Sust. Energy*, **39**, e13297 (2020).

Supporting Information

Exergoeconomic analysis of an LNG integrated - air separation process

Muhammad Haris Hamayun[*,], Naveed Ramzan[*], and Muhammad Faheem[*,†]**

*Department of Chemical Engineering, University of Engineering and Technology, Lahore 54890, Pakistan
**Catalysis and Reaction Engineering Research Group, Department of Chemical Engineering, COMSATS University Islamabad, Lahore Campus, Defence Road, Lahore 54000, Pakistan
(*Received 12 July 2023 • Revised 1 September 2023 • Accepted 2 September 2023*)

Table S1. Operational conditions for the integrated LNG regasification - air separation process

Stream	Flow	Pres.	Temp.	Vapor fraction	Mole fractions								
	TPH	Bar	°C		N_2	O_2	Ar	H_2O	CO_2	CH_4	C_2H_6	C_3H_8	C_4H_{10}
S101	500.00	1.01	25.00	1.00	0.77	0.21	0.01	0.02	0.00	0.00	0.00	0.00	0.00
S102	500.00	2.60	151.93	1.00	0.77	0.21	0.01	0.02	0.00	0.00	0.00	0.00	0.00
S103	500.00	2.50	35.02	1.00	0.77	0.21	0.01	0.02	0.00	0.00	0.00	0.00	0.00
S104	500.00	2.50	35.02	1.00	0.77	0.21	0.01	0.02	0.00	0.00	0.00	0.00	0.00
S105	500.00	6.40	165.68	1.00	0.77	0.21	0.01	0.02	0.00	0.00	0.00	0.00	0.00
S106	500.00	6.30	35.02	0.99	0.77	0.21	0.01	0.02	0.00	0.00	0.00	0.00	0.00
S107	497.56	6.30	35.02	1.00	0.77	0.21	0.01	0.01	0.00	0.00	0.00	0.00	0.00
S111	494.89	6.30	35.02	1.00	0.78	0.21	0.01	0.00	0.00	0.00	0.00	0.00	0.00
S114	158.36	6.30	35.02	1.00	0.78	0.21	0.01	0.00	0.00	0.00	0.00	0.00	0.00
S115	336.53	6.30	35.02	1.00	0.78	0.21	0.01	0.00	0.00	0.00	0.00	0.00	0.00
S116	158.37	6.20	−173.82	0.19	0.78	0.21	0.01	0.00	0.00	0.00	0.00	0.00	0.00
S117	336.53	6.20	−171.73	1.00	0.78	0.21	0.01	0.00	0.00	0.00	0.00	0.00	0.00
S118	158.37	6.10	−174.04	0.19	0.78	0.21	0.01	0.00	0.00	0.00	0.00	0.00	0.00
S119	336.53	6.10	−171.90	1.00	0.78	0.21	0.01	0.00	0.00	0.00	0.00	0.00	0.00
S120	190.73	5.80	−177.07	0.00	1.00	0.00	0.00	0.00	0.00	0.00	0.00	0.00	0.00
S121	304.16	6.05	−172.86	0.00	0.64	0.35	0.01	0.00	0.00	0.00	0.00	0.00	0.00
S122	190.73	5.70	−181.50	0.00	1.00	0.00	0.00	0.00	0.00	0.00	0.00	0.00	0.00
S123	304.16	5.95	−181.50	0.00	0.64	0.35	0.01	0.00	0.00	0.00	0.00	0.00	0.00
S124	190.73	1.50	−192.14	0.11	1.00	0.00	0.00	0.00	0.00	0.00	0.00	0.00	0.00
S125	304.16	1.50	−189.16	0.08	0.64	0.35	0.01	0.00	0.00	0.00	0.00	0.00	0.00
S126	374.82	1.30	−193.34	1.00	0.99	0.00	0.01	0.00	0.00	0.00	0.00	0.00	0.00
S127	374.82	1.20	−175.78	1.00	0.99	0.00	0.01	0.00	0.00	0.00	0.00	0.00	0.00
S128	374.82	1.10	20.43	1.00	0.99	0.00	0.01	0.00	0.00	0.00	0.00	0.00	0.00
S128A	373.92	1.10	20.43	1.00	0.99	0.00	0.01	0.00	0.00	0.00	0.00	0.00	0.00
S128B	0.90	1.10	20.43	1.00	0.99	0.00	0.01	0.00	0.00	0.00	0.00	0.00	0.00
S129	108.73	1.70	−177.97	0.00	0.00	0.99	0.01	0.00	0.00	0.00	0.00	0.00	0.00
S130	108.73	1.60	20.43	1.00	0.00	0.99	0.01	0.00	0.00	0.00	0.00	0.00	0.00
S131A	5.42	1.34	−191.08	0.00	0.70	0.19	0.11	0.00	0.00	0.00	0.00	0.00	0.00
S131B	5.92	1.53	−180.08	0.00	0.02	0.86	0.12	0.00	0.00	0.00	0.00	0.00	0.00
S132	11.34	1.34	−187.53	0.01	0.36	0.53	0.12	0.00	0.00	0.00	0.00	0.00	0.00
S133	11.34	1.24	20.43	1.00	0.36	0.53	0.12	0.00	0.00	0.00	0.00	0.00	0.00
S401	6.00	1.01	−161.72	0.00	0.00	0.00	0.00	0.00	0.00	0.94	0.04	0.01	0.00
S402	6.00	60.00	−158.92	0.00	0.00	0.00	0.00	0.00	0.00	0.94	0.04	0.01	0.00
S403	6.00	59.90	20.43	1.00	0.00	0.00	0.00	0.00	0.00	0.94	0.04	0.01	0.00
S404	6.00	1.20	−118.56	0.98	0.00	0.00	0.00	0.00	0.00	0.94	0.04	0.01	0.00
S405	6.00	1.10	20.43	1.00	0.00	0.00	0.00	0.00	0.00	0.94	0.04	0.01	0.00
S406	6.90	1.10	20.42	1.00	0.08	0.00	0.00	0.00	0.00	0.86	0.04	0.01	0.00

Table S1. Continued

Stream	Flow	Pres.	Temp.	Vapor fraction	Mole fractions								
	TPH	Bar	°C		N_2	O_2	Ar	H_2O	CO_2	CH_4	C_2H_6	C_3H_8	C_4H_{10}
PRG1	0.00	2.50	0.00	0.00	0.00	0.00	0.00	0.00	0.00	0.00	0.00	0.00	0.00
PRG2	2.44	6.30	35.02	0.00	0.00	0.00	0.00	1.00	0.00	0.00	0.00	0.00	0.00
PRG3	2.67	6.30	35.02	0.04	0.00	0.00	0.00	0.96	0.04	0.00	0.00	0.00	0.00
W201	1,961.96	1.01	25.00	0.00	0.00	0.00	0.00	1.00	0.00	0.00	0.00	0.00	0.00
W202	1,961.96	3.30	25.02	0.00	0.00	0.00	0.00	1.00	0.00	0.00	0.00	0.00	0.00
W203A	881.42	3.30	25.02	0.00	0.00	0.00	0.00	1.00	0.00	0.00	0.00	0.00	0.00
W203B	1,080.54	3.30	25.02	0.00	0.00	0.00	0.00	1.00	0.00	0.00	0.00	0.00	0.00
W204	881.42	3.20	40.00	0.00	0.00	0.00	0.00	1.00	0.00	0.00	0.00	0.00	0.00
W205	1,080.54	3.20	40.00	0.00	0.00	0.00	0.00	1.00	0.00	0.00	0.00	0.00	0.00

Table S2. Conditions of heat exchangers used in the integrated process

Heat exchanger	ΔT_{min} (°C)	LMTD (°C)	Duty (kW)
E101	10.00	42.28	16,591
E102	10.00	38.40	20,339
E104	4.29	7.05	36,057
E105	2.92	3.08	1,981

Table S3. Power scenarios of various process equipment in the integrated process

Equipment	Efficiency (%)	Pressure ratio (*)	Power (kW)
K101	72	2.57	17,944
K102	72	2.56	18,491
P201	80	3.26	157.7
P401	80	59.22	27.8
T401	72	50.00	389.8

* Pressure ratio for compressors and pumps is outlet pressure/inlet pressure, while for turbine it is inlet pressure/outlet pressure.

Table S4. Exergy balance across each equipment of the integrated process

Equipment	Exergy balance equation
K101	$E_{S101}+W_{K101}=E_{S102}+E_{d,K101}$
K102	$E_{s104}+W_{K102}=E_{S105}+E_{d,K102}$
E101	$E_{S102}+E_{W203A}=E_{S103}+E_{W204}+E_{d,E101}$
E102	$E_{S105}+E_{W203B}=E_{S106}+E_{W205}+E_{d,E102}$
D101	$E_{S103}=E_{S104}+E_{PRG1}+E_{d,D101}$
D102	$E_{S106}=E_{S107}+E_{PRG2}+E_{d,D102}$
A101	$E_{S107}=E_{S111}+E_{PRG3}+E_{d,A101}$
F101	$E_{S111}=E_{S114}+E_{S115}+E_{d,F101}$
F201	$E_{W202}=E_{W203A}+E_{W203B}+E_{d,F201}$
F401	$E_{S128}=E_{S128A}+E_{S128B}+E_{d,F401}$
P201	$E_{W201}+W_{P201}=E_{W202}+E_{d,P201}$
P401	$E_{S401}+W_{P401}=E_{S402}+E_{d,P401}$
E104	$E_{S114}+E_{S115}+E_{S127}+E_{S129}+E_{S132}+E_{S402}+E_{S404}=E_{S116}+E_{S117}+E_{S128}+E_{S130}+E_{S133}+E_{S403}+E_{S405}+E_{d,E104}$
E105	$E_{S120}+E_{S121}+E_{S126}=E_{S122}+E_{S123}+E_{S127}+E_{d,E105}$
C101	$E_{S118}+E_{S119}+E_Q=E_{S120}+E_{S121}+E_{d,C101}$
C102	$E_{S124}+E_{S125}=E_{S126}+E_{S129}+E_{S131A}+E_{S131B}+E_Q+E_{d,C102}$
T401	$E_{S403}=E_{S404}+W_{T401}+E_{d,T401}$
V101	$E_{S116}=E_{S118}+E_{d,V101}$
V102	$E_{S117}=E_{S119}+E_{d,V102}$
V103	$E_{S122}=E_{S124}+E_{d,V103}$
V104	$E_{S123}=E_{S125}+E_{d,V104}$
M101	$E_{S131A}+E_{S131B}=E_{S132}+E_{d,M101}$
M401	$E_{S405}+E_{S128B}=E_{S406}+E_{d,M401}$